Eur. Phys. J. A 1, 359–364 (1998)

THE EUROPEAN PHYSICAL JOURNAL A

Conversion–electron gamma–ray coincidence spectroscopy of superdeformed ^{135}Nd

B. Aengenvoort[1], W. Korten[1,a], H. Hübel[1], S. Chmel[1], A. Görgen[1], U.J. van Severen[1], W. Pohler[1], R. Zinken[1], T. Härtlein[2], C. Ender[2], F. Köck[2], P. Reiter[2], D. Schwalm[2], F. Schindler[3], J. Gerl[4], R. Schubart[4], F. Azaiez[5], S. Bouneau[5], J. Duprat[5], I. Deloncle[6]

[1] Institut für Strahlen- und Kernphysik, Universität Bonn, Nussallee 14-16, D-53115 Bonn, Germany
[2] Max-Planck Institut für Kernphysik, Saupfercheckweg 1, D-69029 Heidelberg, Germany
[3] Ludwig-Maximilians-Universität München, Am Coulombwall 1, D-85748 Garching, Germany
[4] Gesellschaft für Schwerionenforschung, Planckstr. 1, D-64291 Darmstadt, Germany
[5] Institut de Physique Nucléaire, IN2P3/CNRS, F-91406 Orsay Campus, France
[6] CSNSM, IN2P3/CNRS, F-91405 Orsay Campus, France

Received: 22 December 1997 / Revised version: 19 January 1998
Communicated by B. Herskind

Abstract. Three mini-orange conversion–electron spectrometers and four Euroball Ge Cluster detectors have been used for γ–e$^-$ coincidence spectroscopy of superdeformed ^{135}Nd. Transitions within the superdeformed band are shown to have the expected E2 multipolarity. The 766.5–keV transition which links the band to a positive-parity state has a conversion coefficient consistent with M1 multipolarity. Consequently, positive parity is deduced for the superdeformed band. No evidence for E0 transitions was found.

PACS. 21.10.Hw Spin, parity and isobaric spin – 23.20.Nx Internal conversion and extranuclear effects – 23.20.Js Multipole matrix elements – 27.60.+j $90 \leq A \leq 149$

1 Introduction

Nuclear spectroscopy of high-spin states has made remarkable progress in recent years due to the availability of highly efficient multi-detector γ–ray spectrometers [1-3]. The observational limit for low-intensity transitions has been continuously decreased and detailed investigations of very weak decay channels, like superdeformation, magnetic rotation and band termination, have become possible. On the other hand, the spectroscopy of conversion electrons (CE) is largely missing. The internal conversion process can be dominant for low transition energies and high multipolarities. The conversion coefficients contain information on the electric or magnetic character of the transitions and, thus, determine relative parities of the nuclear states involved. This information can also be obtained from the linear polarization of the γ–rays, but such measurements are time consuming and not suitable for very low γ–ray energies. Furthermore, CE spectroscopy is the only way to detect E0 transitions.

We have performed a measurement of CE in coincidence with γ–rays in ^{135}Nd using a set-up of three mini-orange spectrometers (MOS) [4] and four Euroball Ge Cluster detectors [5]. From CE spectra in coincidence with γ–ray transitions of the superdeformed (SD) band in ^{135}Nd [6,7] we determine conversion coefficients for the in-band transitions and for a linking transition between the band and the normal-deformed states. From these data the parity of a high-spin SD band can be directly determined for the first time. A preliminary report on this work was given earlier [8].

The MOS and Cluster detector set-up is described in the next section, followed by details on the experimental procedure and results in Sect. 3. A discussion of the results follows in Sect. 4.

[a] *Present address:* DAPNIA/SPhN, CEA Saclay, F-91191 Gif-sur-Yvette Cedex, France

2 The mini-orange spectrometers and details of the set-up

The mini-orange filter (MOF) consists of a ring of several permanent magnets which create a thoroidal field to focus electrons within a certain energy range onto a detector [4]. It rejects the large background of low-energy delta electrons which makes in-beam CE experiments so difficult. This arrangement allows to acquire simultaneously CE over a wide energy range without the need for time-consuming field-strength sweeps as with magnetic spectrometers. The compact size of the MOF magnets allows

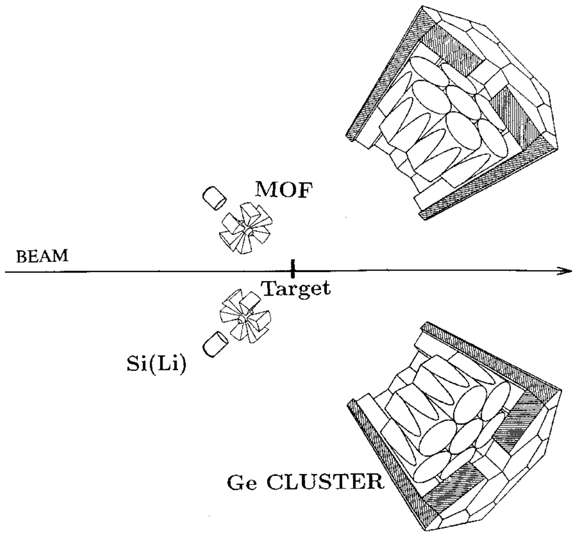

Fig. 1. Schematic drawing of the set-up of three mini-orange spectrometers (MOS) and four Euroball Ge Cluster detectors used in the present work. For clarity only two of the MOS and two of the Cluster detectors are shown

the MOS to be easily integrated into multi–detector γ–ray spectrometers.

The set-up used for our experiment at the Max-Planck Institut für Kernphysik (Heidelberg) is shown schematically in Fig. 1. We have used three MOS positioned at an angle of 137^0 and four Euroball Ge Cluster detectors positioned at 45^0 with respect to the beam.

Each MOF consists of six $SmCo_5$ wedge-shaped magnets of 4.1 cm length and 4.3 cm maximal width surrounding a Pb absorber of 1.5 cm diameter and 3.0 cm length. The radial and azimuthal field strengths measured between the magnets are shown in Fig. 2. The radial field is rather homogeneous, around (85 $\pm$ 10) mT in the center between the magnets. The asymmetry in the azimuthal direction is caused by the use of magnets with alternating strengths.

With this choice of magnets a relatively wide transmission curve (see Fig. 3) is produced that peaks around 600 keV electron energy. The transmission is defined [4] as the number of electrons detected, $N_{MO}(E_e)$, divided by all electrons emitted into the full 4π solid angle, $N_{4\pi}(E_e)$. It has been measured using ^{133}Ba, ^{137}Cs and ^{207}Bi calibration sources.

In each of the MOS a Si(Li) detectors with an active area of 300 mm^2 and a thickness of 3 mm was used. The Si(Li) detectors were cooled to lN_2 temperature. In order to avoid deposits on the cold detector surfaces, each detector had its own vacuum separated from the scattering chamber by an aluminized mylar foil of 360 μg/cm^2 thickness. The deterioration of the energy resolution due to straggeling effects in this foil was negligible compared to other sources (see below). The first stage of the Si(Li) detector preamplifier, consisting of FET, capacitance and feedback resistor, was mounted close to the detector in the cold region. In the calibrations performed in the actual set-up at the accelerator the detectors showed resolutions

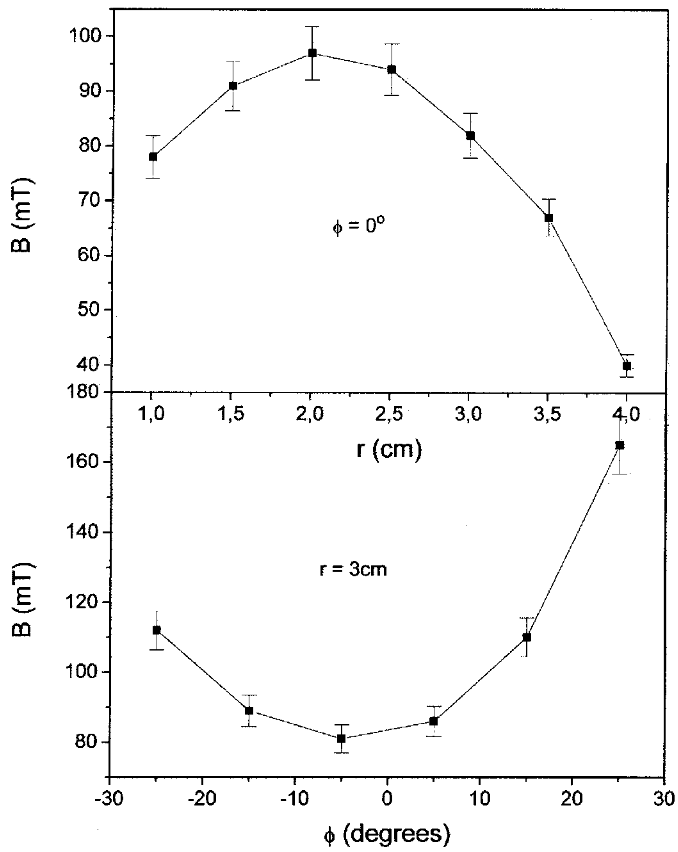

Fig. 2. Magnetic-field strength measured between two of the $SmCo_5$ magnets in radial direction from the center of the MOF (upper part) and azimuthal direction at a distance of 3 cm from the center (lower part)

of 2.9 to 4.0 keV for the 626–keV K-electrons of a ^{137}Cs source.

The center of the MOF magnets had a distance to the target of 8 cm. The Si(Li) detectors were placed 5.3 cm

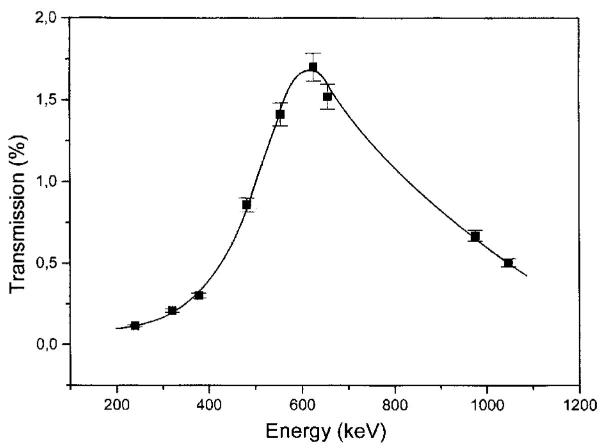

Fig. 3. Transmission $N_{MO}(E_e)/N_{4\pi}(E_e)$ as a function of CE energy of one of the three MOS measured with standard calibration sources. Distances MO - source of 8 cm and MO - detector of 5.3 cm were used. The *curve* is drawn to guide the eye

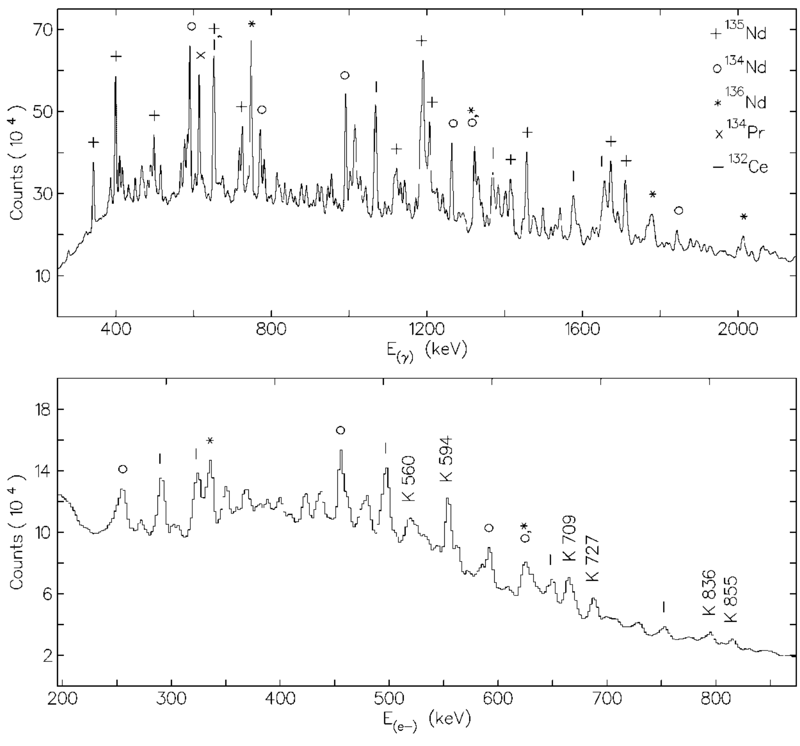

Fig. 4. Total projections of the γ–ray (top) and CE (bottom) coincidences. The energy scale of the CE spectrum is expanded

behind the magnets. Each MOF covers an angular range from 106^0 to 170^0 with respect to the beam axis. In a nuclear reaction with heavy ions the evaporation residues obtain rather large recoil velocities, in our case v/c = 1.4 %. This results in a Doppler–broadening of about 9 keV for CE of 600 keV if the full acceptance range is used. We have therefore limited the angles to larger than 125^0 by mounting a diaphragm before each MOF magnet. This results in a reduction of the Doppler–broadening to about 6 keV, reducing the transmission from its peak value of 1.7 % (see Fig. 3) to 1.3 % for each MOS.

The Cluster detectors [5] were developed for the Euroball project. They consist of seven encapsulated Ge crystals each. Four of these Cluster detectors were mounted at a distance of 26 cm to the target, leading to a solid angle of 3 % of 4π for each Cluster. The total effective photopeak efficiency at a γ–ray energy of 1.3 MeV was 2.6 %. The energy resolution of the individual Ge crystals, measured in the actual set-up at the accelerator, ranged from 2.4 to 2.9 keV at 1.3 MeV.

3 Experimental procedure and results

High-spin states in ^{135}Nd were populated in the reaction ^{124}Te(^{16}O,5n) at a beam energy of 111 MeV. A rather light projectile, ^{16}O, was chosen because it causes a moderate recoil velocity (v/c = 1.4 %) of the ^{135}Nd nuclei. Furthermore, by using a thin target of 300 μg/cm^2 evaporated on a 40 μg/cm^2 Carbon foil the Doppler–broadening due to the velocity spread of the nuclei recoiling into vacuum is minimized. It also keeps the energy straggeling of the CE, which have to pass through the target to reach the MOS, small. The target was enriched in ^{124}Te to 96.7 %. In total about $3 \cdot 10^8$ γ–γ and $1 \cdot 10^8$ CE–γ coincidences were recorded during the experiment. Of the γ–ray coincidences a fraction of 52 % were three- and higher-fold events.

In the off-line analysis the coincidence data were calibrated and sorted into γ–γ and CE–γ matrices. The total projection spectra of the γ–ray and CE coincidences of the two matrices are shown in Fig. 4. They are rather complex as they contain various reaction channels, but nevertheless, several prominent lines can be identified even in the CE spectrum.

Gates were set on all uncontaminated γ–ray transitions of the SD band in ^{135}Nd to obtain single-gated γ–ray and CE spectra. In Fig. 5 the resulting spectra for the γ–rays (top) and the CE (bottom) are displayed. A comparison of these spectra shows that the K-conversion lines of the SD band transitions are clearly observed in the CE spectrum. This spectrum represents the first observation of CE for a high-spin SD band. The K-conversion coefficients obtained from the intensities – corrected for the different detection efficiencies for γ–rays and electrons – are summarized in Table 1. Comparison to theoretical α_K coefficients [9] shows that the measured values are consistent with the expected E2 character of the SD transitions. This result, on the other hand, also constitutes a consistency check of our absolute efficiency calibration for the three MOS.

The SD band decays to the normal-deformed (ND) states via several transitions, as shown in Fig. 6 in which the level scheme of the lower part of the SD band and its decay to the ND states is given. This decay accounts for about 75 % of the intensity of the SD band [7]. The 766.5-keV transition which depopulates the 3324-keV SD state

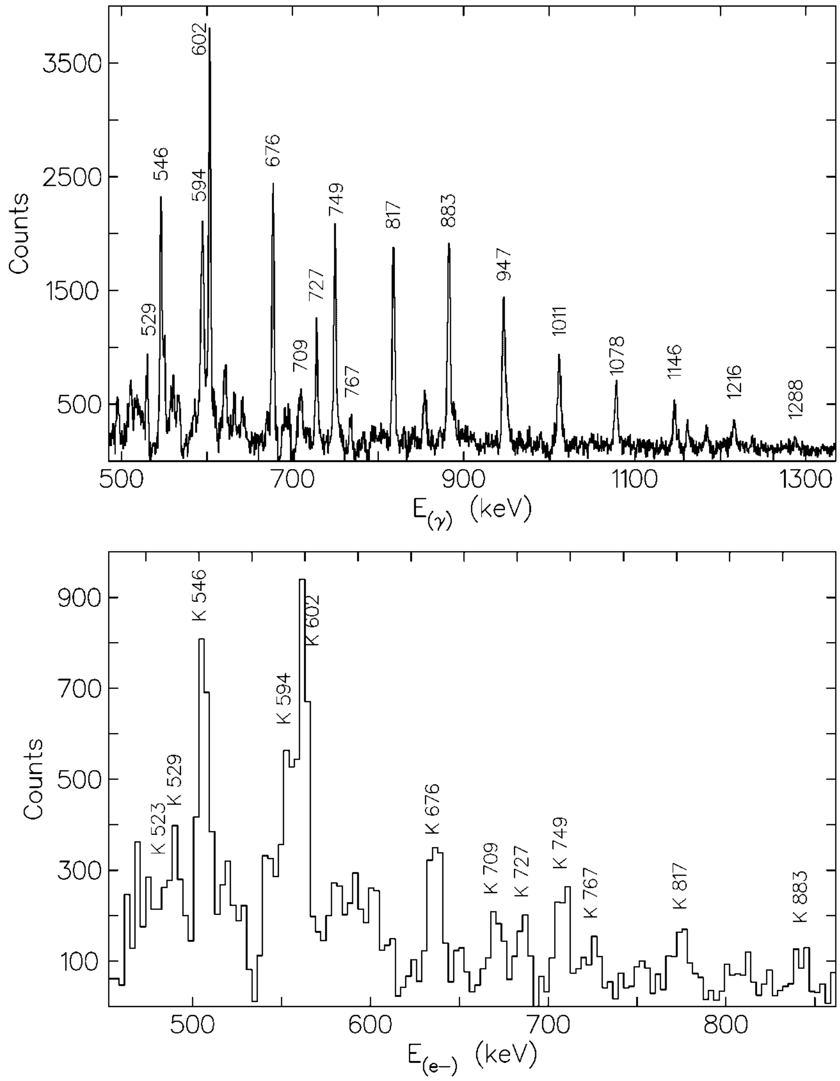

Fig. 5. Spectra of γ–rays (top) and conversion electrons (bottom) taken in coincidence with γ–ray transitions in the superdeformed band of ^{135}Nd. The energy scale of the CE spectrum is expanded in the range of interest

Table 1. Experimental and theoretical K-conversion coefficients for transitions in ^{135}Nd

Energy [keV]	α_K^{exp} $[\cdot 10^{-3}]$	α_K^{theo} $[\cdot 10^{-3}]$	Multipolarity
SD transitions			
545	7.1±1.3	7.8	E2
676	4.3±0.8	5.2	E2
749	3.6±0.7	3.8	E2
817	2.9±0.6	3.1	E2
883	2.1±0.5	2.7	E2
linking transition			
766.5	7.5±2.2	5.6	M1
		1.4	E1
523.5	8.0±6.2[a]	14.6	M1
		9.0	E2

[a] using intensity branching ratios given in [7]

and feeds into the $23/2^+$ level at 2557 keV has a DCO ratio of a stretched dipole [7]. It is the only transition in the sensitive range of the MOS that is well separated in energy from other transitions. It may therefore be used to determine the parity of the SD band if we can distinguish between electric and magnetic character of this transition. The 766.5-keV transition lies close to the 748.3-keV SD transition and to the 727.0-keV E2 transition of the negative-parity ND band (see Fig. 6). Comparison of the CE and γ–ray intensities of these transitions gives, after proper correction for the efficiencies and angular distributions, the K-conversion coefficient of the 766.5-keV transition. The result is also included in Table 1. Within its experimental uncertainty it is compatible with M1 multipolarity while it is much larger than that for E1 multipolarity. Therefore we adopt positive parity for the SD band.

In the decay between states of different deformation E0 transitions may occur [12-16]. We have searched for an E0 admixture to the 523.5-keV ΔI = 0 transition, but within our accuracy no excess electron intensity was found (see Table 1). We have also made a survey of all CE transitions in the spectrum in coincidence with the SD band, but do not find any lines that are not accounted for by known transitions.

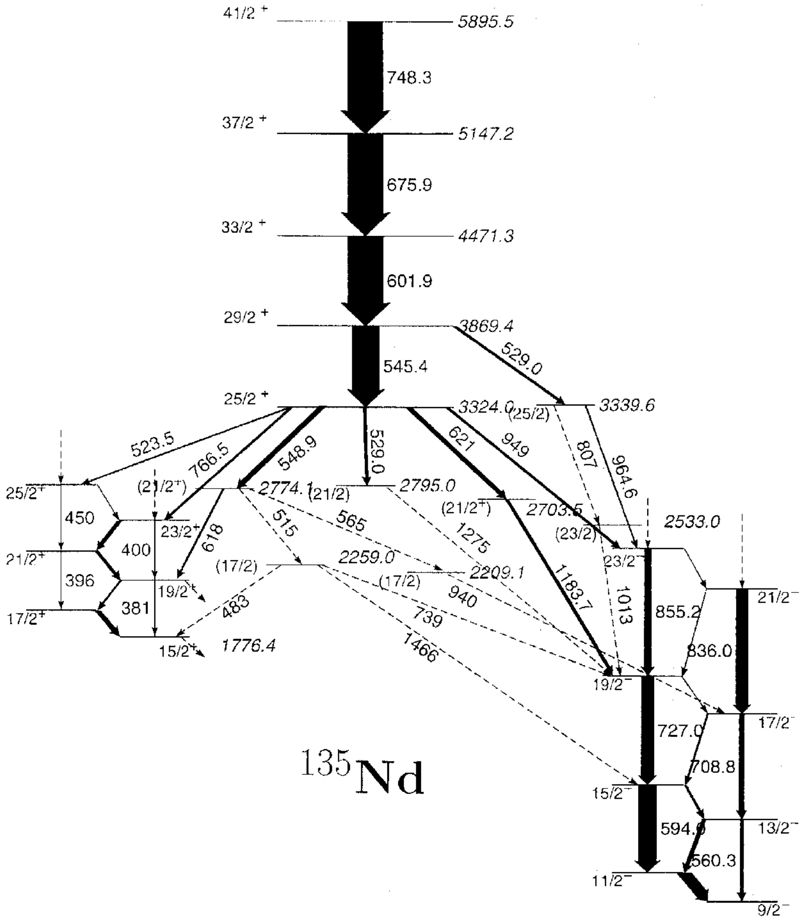

Fig. 6. Partial level scheme of ^{135}Nd showing the bottom part of the SD band and its decay to the normal-deformed states [7]. The parity of the SD band is determined in the present work

4 Discussion

For ^{135}Nd with neutron number N = 75 at large prolate deformation the positive-parity Nilsson orbital [660]1/2 of $i_{13/2}$ origin (6_1) lies close to the Fermi surface. It is strongly deformation-driving and, thus, has been suggested to be mainly responsible for the SD bands of nuclei in the mass-130 region. Our experimental result that the SD band in ^{135}Nd has positive parity confirms this suggestion. It is the first direct determination of the parity of a SD band and is of importance for the SD bands for this whole mass region.

The SD band shows a highly fragmented decay into the ND states. This decay pattern and the measured lifetimes [11] suggest that the band ceases to exist at the 3324-keV level. Total routhian surface calculations [7] for the positive parity, positive signature configuration, keeping the odd neutron always in the 6_1 level, show two competing minima in the frequency range of 0.15 to 0.25 MeV. The one representing the SD band with $\beta = 0.35$ and $\gamma = 8^o$ is the lowest for high frequencies. The second minimum is strongly triaxial ($\beta = 0.25$, $\gamma = 30^o$) and is lowest at $\hbar\omega = 0.15$ MeV. Between 0.15 and 0.20 MeV both minima have the same energy with only a shallow barrier between them. It was therefore suggested [7] that with decreasing rotational frequency the nucleus changes from the high- to the low-deformation minimum, resulting in the observed termination of the SD band. The transition quadrupole moments derived from the lifetime measurements in the decay region [11] are in accordance with this interpretation. The decrease of Q_t between the 601.9, 545.4 and 621-keV transitions may be understood within a scenario in which the $29/2^+$ state is superdeformed, the 3324 MeV $25/2^+$ level is a mixture of low and high deformation with about equal amplitudes and the $21/2^+$ states have a low deformation.

Transitions between states of different deformation which are highly mixed are expected to show an enhanced E0-decay probability [12,13]. However, in our experiment we did not find any evidence for E0 transitions. Therefore, we want to investigate the competition between E0 and the normal decay modes of the SD band in a more quantitative way. The 523.5-keV $25/2^+ \rightarrow 25/2^+$ transition in the decay of the SD band, see Fig. 6, is a good candidate for a search for an E0 admixture. The E0-decay rate, corresponding to the emission of K, L_I, L_{II}, ... electrons, can be written as [16, equ. A2]

$$\lambda_{E0} \; = \; 2.786 \cdot 10^{20} \; \frac{E_\gamma}{2\,I\,+\,1} \; A(E0)\;\rho^2(E0) \qquad (1)$$

where E_γ is the transition energy in MeV and $A(E0)$ is in natural units as tabulated in [15]. Assuming two-level mixing between states of different deformation, ρ(E0) is given by [12-14]

$$\rho(E0) \;=\; \frac{3\;Z}{4\;\pi}\;a\;b\;(\beta^2_{(1)} - \beta^2_{(2)}). \qquad (2)$$

Here, $\beta_{(1)}$ and $\beta_{(2)}$ are the deformations and a and b the mixing amplitudes of the initial and final states, respectively. The deformation of the SD band may be obtained from the experimental B(E2) values [10,11], $\beta_{(1)} = 0.37$. For the normal states we adopt $\beta_{(2)} = 0.20$ calculated by Möller et al. [17] for the ground state. With these parameters we obtain an upper limit of ρ(E0) = 0.69 if we assume maximal mixing, $a \cdot b = 0.5$. A large mixing seems reasonable considering the decay pattern of the SD band discussed above.

Using (1) and this value for ρ(E0) we obtain an upper limit for the E0-decay rate of the 523.5-keV transition of

$$\lambda_{E0} \;=\; 2.57 \cdot 10^8\; s^{-1}.$$

An estimate of the E0 admixture to the K line of the 523.5-keV transition may be obtained in the following way. In principle, it may be of mixed E0 + M1 + E2 character. The total probability for the emission of CE is then

$$\lambda_e \;=\; \lambda_{E0} \;+\; \lambda_\gamma[\alpha(M1)\frac{1}{1+\delta^2} \;+\; \alpha(E2)\frac{\delta^2}{1+\delta^2}] \qquad (3)$$

where α(M1) and α(E2) are the M1 and E2 conversion coefficients, respectively, and δ^2 is the E2/M1 mixing ratio. In the following we assume that the E2 admixture is small ($\delta^2 \approx 0$). The M1 γ–ray transition probability λ_γ can then be obtained from the measured lifetime of the $25/2^+$ level at 3324 keV, $\tau = 2.4(9)$ ps [11], and the intensities of the different decay branches given by Deleplanque et al. [7]. If we, furthermore, take the 16 % branch of unobserved transitions into account, we obtain λ_γ(524 keV) $\approx 3.25 \cdot 10^{10}$ s^{-1}. For the contribution to the K-conversion line one then obtains

$$\lambda_{e,M1} \;=\; \lambda_\gamma \alpha(M1) \;\approx 4.7 \cdot 10^8\; s^{-1}.$$

This result shows that the decay rate for M1 CE is much larger than that for E0 decay, in particular as the E0 rate estimated above is an upper limit. Although the E0 strength ρ(E0) can be rather large for large mixing of the SD and ND states, the E0 branching is small because of the relatively low Z of 60 for ^{135}Nd and the rather large spin of 25/2 at which the SD band decays to the yrast states. It is therefore not surprising that we do not find a sizeable E0 admixture in the 523.5-keV K-line in our experiment.

The support of the German Euroball Collaboration in the development and setting up of the Cluster detectors is gratefully acknowledged. This work was supported by BMBF.

References

1. C.W. Beausang and J. Simpson, J. Phys. G **22**, 527 (1996)
2. D. Bazzacco, Proc. Int. Conf. on Nucl., Structure at High Angular Momentum, Ottawa (1992), Vol.2, Proc. AECL 10613, p. 376
3. I.Y. Lee, Nucl. Phys. A **520**, 641c (1990)
4. J. van Klinken and K. Wisshek, Nucl. Instr. and Meth. **98**, 1 (1972)
5. J. Eberth, Prog. Part. Nucl. Phys. **28**, 495 (1992)
6. E.M. Beck, F.S. Stephens, J.C. Bacelar, M.A. Deleplanque, R.M. Diamond, J.E. Draper, C. Duyar and R.J. McDonald, Phys. Rev. Lett. **58**, 2182 (1987)
7. M.A. Deleplanque, S. Frauendorf, R.M. Clark, R.M. Diamond, F.S. Stephens, J.A. Becker, M.J. Brinkmann, B. Cederwall, P. Fallon, L.P. Farris, E.A. Henry, H. Hübel, J.R. Hughes, W. Korten, I.Y. Lee, A.O. Macchiavelli, M.A. Stoyer, P. Willsau, J.E. Draper, C. Duyar and E. Rubel, Phys. Rev. C **52**, R2302 (1995)
8. W. Korten, B. Schulze, H. Hübel, S. Chmel, A. Görgen, U.J. van Severen, W. Pohler, R. Zinken, T. Härtlein, C. Ender, F. Köck, P. Reiter, D. Schwalm, F. Schindler, J. Gerl, R. Schubart, F. Azaiez, S. Bouneau, J. Duprat, I. Deloncle, Z. Phys. A **358**, 217 (1997)
9. F. Rösel, H.M. Fries, K. Alder and H.C. Pauli, Atomic Data Nucl. Data Tables **21**, 91 (1978)
10. R.M. Diamond, C.W. Beausang, A.O. Macchiavelli, J.C. Bacelar, J. Burde, M.A. Deleplanque, J.E. Draper, C. Duyar, R.J. McDonald and F.S. Stephens, Phys. Rev. C **41**, R1327 (1990)
11. P. Willsau, H. Hübel, R.M. Diamond, M.A. Deleplanque, A.O. Macchiavelli, J.R. Oliveira, F.S. Stephens, H. Kluge, J.A. Becker, E.A. Henry, A. Kuhnert and M. Stoyer, Phys. Rev. C **48**, R494 (1993)
12. K. Heyde and R.A. Meyer, Phys. Rev. C **37**, 2170 (1988)
13. J.L. Wood, E.F. Zganjar and K.Heyde, Z. Phys. A **353**, 355 (1996)
14. R. Krücken and I.Y. Lee, Phys. Rev. C **55**, R2760 (1997)
15. R.S. Hager and E.C. Seltzer, Nucl. Data Tables A **6**, 1 (1969)
16. J.X. Saladin, M.P. Metlay, D.F. Winchell, M.S. Kaplan, I.Y. Lee, C. Baktash, M.L. Halbert, N.R. Johnson and O. Dietzsch, Phys. Rev. C **53**, 652 (1996)
17. P. Möller, J.R. Nix, W.D. Myers and W.J. Swiatecki, Atomic Data Nucl. Data Tables **59**, 185 (1995)